

Catalysis Science & Technology

Accepted Manuscript



This is an *Accepted Manuscript*, which has been through the Royal Society of Chemistry peer review process and has been accepted for publication.

Accepted Manuscripts are published online shortly after acceptance, before technical editing, formatting and proof reading. Using this free service, authors can make their results available to the community, in citable form, before we publish the edited article. We will replace this *Accepted Manuscript* with the edited and formatted *Advance Article* as soon as it is available.

You can find more information about *Accepted Manuscripts* in the [Information for Authors](#).

Please note that technical editing may introduce minor changes to the text and/or graphics, which may alter content. The journal's standard [Terms & Conditions](#) and the [Ethical guidelines](#) still apply. In no event shall the Royal Society of Chemistry be held responsible for any errors or omissions in this *Accepted Manuscript* or any consequences arising from the use of any information it contains.

Transition-state scaling relations in zeolite catalysis: influence of framework topology and acid-site reactivity

Chuan-Ming Wang^{1,2}, Rasmus Y. Brogaard^{2,3}, Zai-Ku Xie^{1*}, Felix Studt^{2*}

¹ SINOPEC Shanghai Research Institute of Petrochemical Technology, Shanghai 201208, China

² SUNCAT Center for Interface Science and Catalysis, SLAC National Accelerator Laboratory, CA 94025, USA, and Department of Chemical Engineering, Stanford University, CA 94305, USA

³ inGAP Center for Research Based Innovation, Department of Chemistry, University of Oslo, Norway.

* Corresponding author. E-mail: studt@slac.stanford.edu; xzk@sinopec.com

Abstract:

Microporous acid catalysts are extensively used in the chemical industry because of their high activity and unique shape-selectivity induced by frameworks with molecular-sized voids. However, it remains a challenge to tailor catalytic activity by choice of pore structure and acid strength. In this theoretical work we aim at extracting trends in how zeotype-catalyzed reactions are influenced by reactivity of Brønsted acid sites and framework topology. Using olefin-methanol reactions as an example, we consider a number of elementary steps across 21 zeotype materials of three different topologies. Density Functional theory was employed to calculate the enthalpies of transition states (TSs) and establish scaling relations across catalyst acid strength and framework topology, using the ammonia heat of adsorption as a descriptor of acid-site reactivity. The results indicate that when cation-like TSs are increasingly stabilized by dispersion interactions with the framework, they become less sensitive to changes in the reactivity of acid sites. It is crucial to further investigate this finding to ultimately be able to tailor the activity of zeotype acid catalysts, appreciating the influence of both framework topology and acid strength.

Keywords: zeolite catalysis, aluminophosphates, density functional theory, scaling relations, acid strength, framework topology, olefin methylation

Introduction

Zeolites and zeotypes with well-defined microporous crystalline structures are widely used in the chemical industry where they catalyze a variety of important reactions, such as fluid catalytic cracking (FCC), toluene disproportionation, aromatic alkylation, or methanol to hydrocarbons (MTH) conversions.¹⁻⁴ In solid acid catalysis involving zeolites, catalytic activity and selectivity are determined by acid strength as well as framework topology.⁵⁻⁹ Several experimental and theoretical works have investigated how intermediates and transition states (TSs) are stabilized by interaction with the acid site and confinement by the surrounding framework.⁸⁻¹³ The reaction rates generally increase with acid strength and confinement, but it remains unclear how to specifically tailor framework and acidity of zeolites to improve catalytic activity. In this theoretical work we consider a large number of materials, to extract trends in how the topology and properties of the acid site affect zeotype-catalyzed reactions between olefins and methanol.

In catalysis involving metal (oxide) surfaces, new catalysts have successfully been designed by identifying key descriptors determining catalytic activity and selectivity.¹⁴⁻¹⁹ Similar structure-activity relationships have been investigated in zeolite catalysis.²⁰⁻²³ When using zeolites and other solid Brønsted acids as catalysts it is a central challenge to quantify the acidity of the material.²⁴ The deprotonation energy (DPE) represents a rigorous measure of intrinsic acid *strength*.^{7,11,21,23,25,26} However, recent works indicate that DPE is an incomplete descriptor of the acid-site *reactivity* that determines catalytic activity of solid acids.^{23,27} Experimentally, zeolite acid strength is often quantified through the adsorption enthalpy of bases, typically ammonia or organic amines.^{28,29} In a computational investigation, Borges et al. observed a linear relationship between the adsorption enthalpy of ammonia (ΔH_{NH_3}) and the activation energy of alkane cracking at models of zeolite acid sites.²⁰ We employed ΔH_{NH_3} in a descriptor-based approach to elucidate how the reactivity of Brønsted acid sites affects the rate of olefin-methanol reactions in zeotype catalysts.^{27,30} ΔH_{NH_3} was used as a quantitative descriptor of acid-site reactivity, as it was found to capture the interactions of reaction intermediates and TSs with the acid site of the catalyst.^{27,30} Linear enthalpy scaling relations with ΔH_{NH_3} were established for each species in the reaction

network and the scaling relations were used in micro-kinetic modeling of reaction rates, establishing a quantitative relation between catalytic activity and acid-site reactivity.

Our previous work hence provides a protocol for screening zeotype catalysts of the CHA/AlPO-34 framework topology.^{27,30} However, as our ultimate aim is to extract general trends in zeotype acid catalysis, it is crucial to investigate how our descriptor-based approach can be employed across multiple framework topologies. In this work we established scaling relations of TS enthalpies in zeotype acid catalysts of three different topologies, again using olefin methylation as a case study. Together with previous work,^{27,30} the results indicate that the scaling relations with acid-site reactivity hold for zeolite-catalyzed olefin-methanol reactions in CHA, AEI, and AFI frameworks. In addition, the results suggest that cation-like molecular species are less sensitive to acid-site reactivity the more they are stabilized by the surrounding framework.

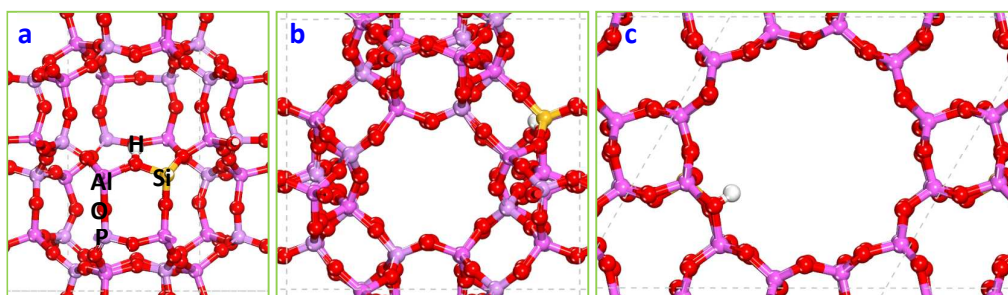


Figure 1. Optimized structures of (a) Si-AlPO-34, (b) Si-AlPO-18, and (c) Si-AlPO-5 exhibiting the framework structures of AlPO-34/CHA, AlPO-18/AEI, and AlPO-5/AFI.

Results and Discussion

Three different zeotype topologies (AlPO-34/CHA, AlPO-18/AEI, and AlPO-5/AFI) exhibiting different channel and cavity structures were investigated (see Figure 1).³¹ Similar to our earlier studies,^{27,30} we modulate the acid strength by isomorphous substitution of one Si atom by Me(III) atoms (Al, Ga) in the silicate zeolites investigated here. Analogously, the P and Al atoms of aluminophosphates were substituted by Me(IV) and Me(II) atoms, respectively. We chose Si, Ge, and Ti for the Me(IV) and Mg and Zn for the Me(II) substitution.

We use the same nomenclature as in previous works,^{27,30} and Al-CHA, Al-AEI and Al-AFI are hence the well-known zeolites H-SSZ-13, H-SSZ-39, and H-SSZ-24. As in earlier work we used periodic density functional theory (DFT) calculations employing the Bayesian Error Estimation Functional with van der Waals (vdW) correlation (BEEF-vdW).³² This functional has been shown to quantitatively capture the vdW interactions of alkane adsorption and olefin methylation kinetics in the Al-TON zeolite.^{33,34} The computational setup is identical to the one described previously and briefly outlined in the methods section.^{27,30}

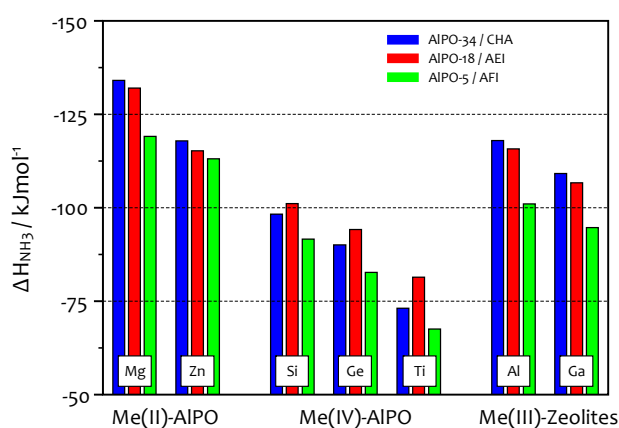
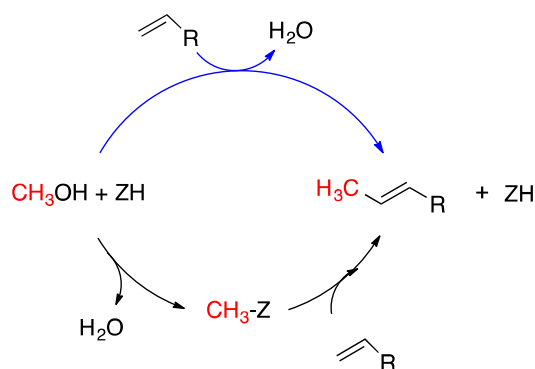


Figure 2. Calculated adsorption enthalpies of ammonia in isomorphically substituted zeolites and zeotype materials. The values in Me-AIPO-34/CHA are taken from Reference²⁷.

Figure 2 shows the calculated ΔH_{NH_3} of different metal-substituted zeotypes (the values are listed in Table S3). For the zeotypes investigated here, we find that the reactivity as measured by ΔH_{NH_3} decreases in the order Mg, Zn (Me(II) substitution), Al, Ga (Me(III) substitution), Si, Ge, Ti (Me(IV) substitution). The reactivity spans up to 60 kJ/mol of calculated ΔH_{NH_3} between the most reactive and least reactive zeotypes. When substituting the same element in the different frameworks investigated here, the differences are up to 20 kJ/mol. The acid-site reactivity hence depends on the framework topology, although substitution can change reactivity even more. A similar picture emerges when considering acid strength: in Al-zeolites of MFI, MOR, CHA, and FAU topologies calculated DPE values span 30 kJ/mol,²⁵ while in zeolites of the same topology (Me-MFI, Me=Al, Ga, Fe, B) the calculated DPE values span 80 kJ/mol.¹³ The calculated ΔH_{NH_3} of HSSZ-13 (-118 kJ/mol)

compares quite well with the experimentally determined value of -131 kJ/mol ,³⁵ considering that the accuracy of DFT is usually about $\pm 20 \text{ kJ/mol}$. Even considering this error, we note that recent work has shown that trends across different materials are usually well preserved.³⁶ Moreover, the BEEF-vdW functional is able to capture the relative trends observed experimentally with ΔH_{NH_3} increasing from Si-AlPO-5 to Si-AlPO-34.³⁷

AlPO-34/CHA and AlPO-18/AEI have cavities interconnected by eight-membered ring pores with similar size ($3.8 \text{ \AA} \times 3.8 \text{ \AA}$).³¹ Their acid-site reactivities, as measured by ΔH_{NH_3} , are therefore similar when substituted by the same atom. AlPO-5/AFI, on the other hand, possesses one-dimensional twelve-membered channels ($7.3 \text{ \AA} \times 7.3 \text{ \AA}$, see Figure1).³¹ The reactivities of the acid sites within Me-AlPO-5/AFI are therefore apparently different from those found for the other two topologies.



Scheme 1. Reaction between methanol and olefins catalyzed by zeolites through the concerted (blue) or stepwise (black) pathway.

We will now move on to consider a catalytic reaction across the different frameworks and acid sites. As in previous studies we will use the methanol-ethene and methanol-propene reactions as examples. Both methylation reactions are important steps in the methanol-to-olefins (MTO) process.³⁸⁻⁴⁹ The MTO process has been shown to proceed through the dual-cycle hydrocarbon pool mechanism, in which the methylation of aromatics or olefins contributes to the growth of (side) chains, which is then followed by elimination or cracking steps to form products.^{39,45,50,51} There is broad agreement in the field that

methylation can proceed through either the concerted or stepwise mechanisms, as shown in Scheme 1.^{34,52-56} In the concerted pathway, the adsorbed methanol reacts directly with the olefin in a single step, whereas in the stepwise pathway a surface-bound methyl group is first formed and then reacts with the olefin. The preferred pathway depends on the reaction conditions, olefin sizes and catalyst material.^{34,52-56} It has been predicted that in H-SSZ-13 the stepwise mechanism dominates for smaller olefins.^{27,30} In this work we consider both pathways for the methylation of propene. For ethene methylation we only address the reaction proceeding through the concerted pathway, in order to limit the already massive demand on computational resources of this work. We emphasize that this work uses olefin-methanol reactions to illustrate our descriptor-based approach, not aiming to predict kinetic parameters of the reactions.

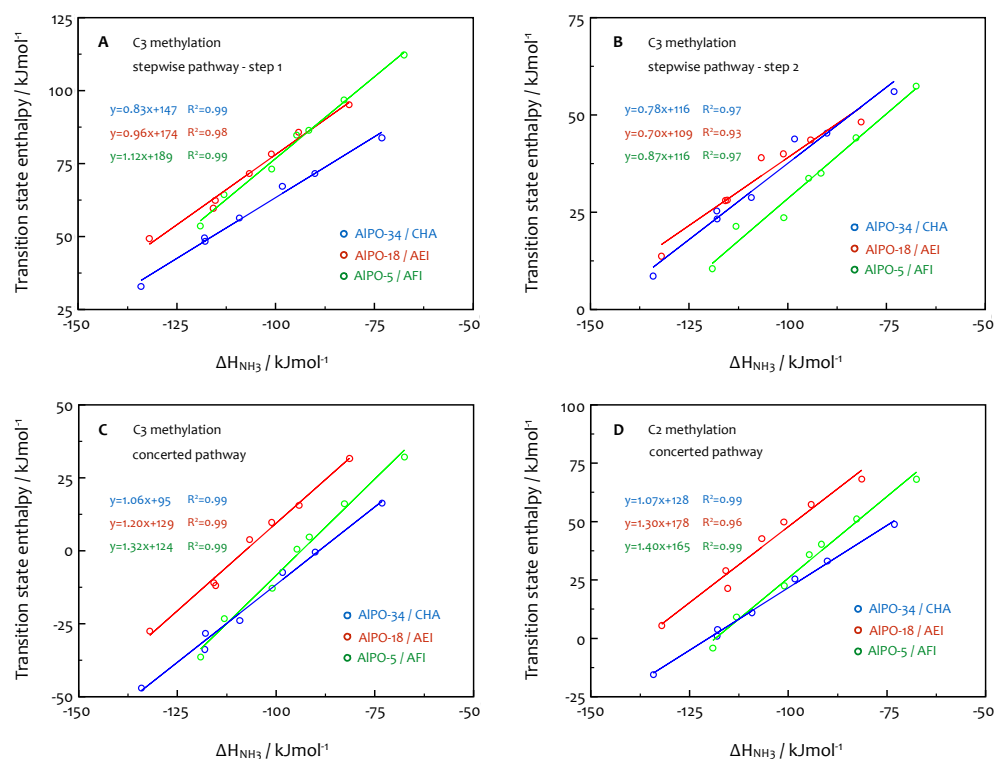


Figure 3. Linear scaling relations between the calculated transition-state enthalpies (relative to the gas-phase reactants) and the calculated ammonia heat of adsorption, ΔH_{NH_3} , for (A) the first step of the stepwise pathway in the reaction between methanol and propene, (B) the second step of the stepwise pathway in the reaction between methanol and propene, (C) the

concerted pathway in the reaction between methanol and propene, and (D) the concerted pathway in the reaction between methanol and ethene. Blue circles represent scaling in the AlPO-34/CHA framework, red circles in the AlPO-18/AEI framework, and green circles in the AlPO-5/AFI framework. Data for AlPO-34/CHA is taken from Reference²⁷.

As previously reported for AlPO-34/CHA,^{27,30} we were able to establish scaling relations between the TS enthalpies of the stepwise and concerted pathways and the ammonia heat of adsorption for AlPO-18/AEI and AlPO-5/AFI (see Figure 3). The TS enthalpy is shown relative to methanol and the olefins in the gas phase (see Scheme S1). We have used the same reference state in previous works,^{27,30} as it allows to compare stabilities of intermediates and TSs on the same footing. We note that the correlation in the scaling relations is remarkably strong. Note in particular that for a given species both zeotypes and zeolites fall on the same scaling line. As suggested previously, this strongly indicates that the sum of the interactions between a given species and the framework is virtually identical in both aluminophosphates and zeolites.^{27,30} Interestingly, the relative enthalpies of TSs in the concerted pathway for propene and ethene methylation can be predicted using a simple formula which is linearly fitted using two variables (ΔH_{NH_3} and number of C atoms in olefins) from the calculated results as shown in Figure 4. The enthalpies of TSs involving ethene are about 30 - 40 kJ/mol higher than those involving propene, as found in previous work.³⁰ This qualitatively agrees with experimental findings that the rate of propene methylation is systematically higher than ethene methylation across a range of frameworks.^{41,42,49} A number of computational works derived rate constants for the reaction between adsorbed methanol and gas phase olefins in a series of zeolite frameworks.^{40,44,57} The authors arrived at activation energies for ethene that were 20 - 30 kJ/mol higher than for propene, agreeing well with the relative TS enthalpies found in the present work.

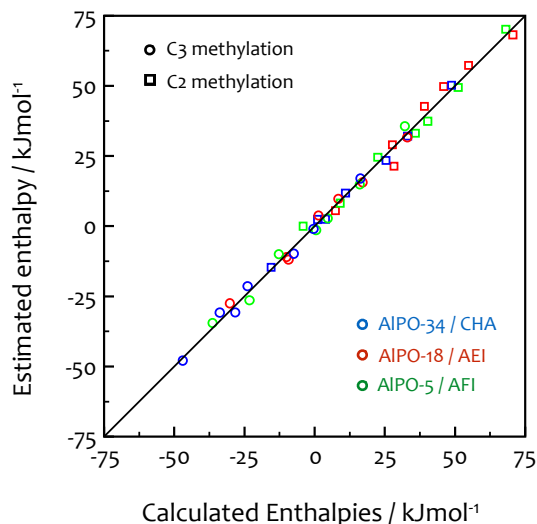


Figure 4. Estimated transition state enthalpies plotted against the calculated values for propene (circles) and ethene (squares) methylation through the concerted pathway in AIPO-34/CHA (blue), AIPO-18/AEI (red), and AIPO-5/AFI (green) frameworks. Estimated values are derived using $\Delta H^{\text{TS}} = 1.07\Delta H_{\text{NH}_3} - 33n + 195$ (AIPO-34/CHA), $\Delta H^{\text{TS}} = 1.25\Delta H_{\text{NH}_3} - 38n + 248$ (AIPO-18/AEI), and $\Delta H^{\text{TS}} = 1.36\Delta H_{\text{NH}_3} - 35n + 231$ (AIPO-5/AFI), where n is the number of C atoms in the corresponding olefin. The mean absolute error resulting from these predictions are 1.5, 2.5, and 2.4 kJmol^{-1} , for AIPO-34/CHA, AIPO-18/AEI, and AIPO-5/AFI, respectively.

We note that the slopes of the scaling relations depend on the type of framework. For the TSs investigated the slope of the scaling decreases in the order: AIPO-5/AFI > AIPO-18/AEI > AIPO-34/CHA, except in the second step of the stepwise pathway. For the latter TS, the slope is less sensitive to the type of framework and the linear correlation is not as good as the other TSs. This could indicate that the TS of stepwise methylation resembles an ion-pair to a lesser extent than the TS for concerted methylation does, as discussed previously.³⁰ We further note that this TS might present a limiting case for the use of ammonia as a probe; one might have to choose other molecules representing the interaction between the zeotype and the TS more accurately.

We now focus on the TSs for concerted methylation and methoxy formation, respectively.

In a simple picture, these species are ion-pairs embedded in a polarizable medium constituted by the framework. It has been shown that ion-pair interactions are weakened when two charges of opposite sign are situated in a polarizable lattice.⁵⁸ This leads us to suggest that dispersion interactions with the zeotype framework weaken the interactions between cation-like species and the deprotonated acid site. This hypothesis is addressed in the following.

Table 1. Slopes of scaling relations for olefin methylation and adsorption energies of propene, ethene, and fitted CH₂ group in three framework topologies.

		Me-AIPO-34/CHA	Me-AIPO-18/AEI	Me-AIPO-5/AFI
Slope	C3 methylation: Concerted	1.06 ± 0.05	1.20 ± 0.05	1.32 ± 0.07
	C3 methylation: Stepwise 1 st step	0.83 ± 0.04	0.96 ± 0.05	1.12 ± 0.05
	C3 methylation: Stepwise 2 nd step	0.78 ± 0.06	0.70 ± 0.08	0.87 ± 0.06
	C2 methylation: Concerted	1.07 ± 0.03	1.30 ± 0.10	1.40 ± 0.07
Adsorption energy ^[a]	Fitted CH ₂ group ^[b]	-13.9 ± 0.5	-10.8 ± 0.2	-7.5 ± 0.4
	Propene ^[c]	-49 ± 2	-42 ± 3	-39 ± 1
	Ethene ^[c]	-36 ± 1	-29 ± 3	-27 ± 1

[a] All energies are in kJ/mol. [b] Data estimated from a linear fit of physisorption energies of methane to butane in the corresponding AIPO frameworks (see Figure S1). [c] Adsorption energies of ethene or propene were averaged over each framework with different isomorphous substitution (see Table S4 and S5) in which methanol is adsorbed at the Brønsted acid site.

Recent work demonstrated that dispersion interactions, quantified using DME as a probe, stabilize TSs in condensation of methanol to dimethyl ether (DME) in a series of zeolite frameworks.¹¹ In this work we quantify dispersion interactions in two ways. First, through physisorption enthalpies of linear alkanes, that scale linearly with the number of carbon atoms in the molecule.^{33,59,60} We have calculated physisorption energies of linear alkanes in AIPO-34, AIPO-18, and AIPO-5, finding that the energy decreases by 14, 11, and 8 kJ/mol per carbon atom, respectively (see Figures 1 and S1). Second, we quantify dispersion interactions through the co-adsorption energies of propene and ethene, respectively, with methanol (see Table 1). These adsorption energies compare well with the values of -37 and

-53 kJ/mol calculated for ethene and propene, respectively, using PBE-D in periodic Al-MFI model.⁴⁰ In silicalite-1, the siliceous analogue to Al-MFI, heats of physisorption were measured to -24 ~ -31 and -40 kJ/mol for ethene and propene, respectively.⁶¹ As summarized in Table 1, S3 and S4, the co-adsorption energies decrease by framework in the same order as the alkane physisorption energies. Hence, the two measures agree that dispersion stabilization by the framework decreases in the order AlPO-34/CHA > AlPO-18/AEI > AlPO-5/AFI.

Returning to the TSs for the concerted methylation and methoxy formation, Table 1 supports our hypothesis: when species are more stabilized by the framework (stronger CH₂ adsorption) they are less sensitive to changes in the acid-site reactivity (lower scaling slope). This can influence the relative rates of parallel reactions in a catalytic process; if reaction A involves (large) species that are heavily stabilized by the framework and reaction B does not, a change in acid-site reactivity will influence the rate of reaction B more than that of A. It is an intriguing thought to exploit this phenomenon in the design of catalytic materials, to favor the target reaction over unwanted parallel reactions by tuning acid strength.

Conclusion

This work aimed at extracting trends in how framework topology and acid-site properties affect zeotype-catalyzed reactions, taking olefin-methanol reactions as an example. Together with previous work, we have established enthalpy-scaling relations for transition states in propene and ethene methylation with ΔH_{NH_3} as a descriptor of acid-site reactivity in 21 zeotype catalysts, comprising 7 acid sites and three different framework topologies. The results promise that our descriptor-based approach has potential as a general way of extracting trends in zeolite acid catalysis, as it has now been shown to work across multiple reactions, acid sites and zeotype frameworks.

The results of this work qualitatively indicate that when cation-like species are more stabilized by the framework, they are less sensitive to changes in acid-site reactivity. This raises the interesting question of whether it is possible to change the relative rates of two reactions enhanced to different extents by the framework, by exploiting that a change in

acid-site reactivity would influence one reaction more than the other.

Methods

The computational setup is identical to that used in previous work.^{27,30} Briefly, all density functional theory (DFT) calculations were carried out using the GPAW package, a real-space grid implementation of the projector augmented-wave method.^{62,63} A grid spacing of 0.20 Å in real-space was used. The Brillouin zone was sampled only with the Γ point. The Bayesian error estimation functional with van der Waals correlation (BEEF-vdW) was employed.³² The climbing image nudged elastic band (CI-NEB) method was used to locate all the transition states.⁶⁴ A force threshold of 0.03 eV/Å for transition states and 0.01 eV/Å for other states like intermediates was used in these calculations. The vibrational frequency calculations employing a partial Hessian approach (H atom of acidic site, and involved organic species). In each of the three considered topologies a frequency calculation was performed for each species in the Si-AlPO structure, in order to correct zero-point energies (ZPE) and calculate enthalpies. The correction energies were then reused for other materials of the same topology, assuming that the corrections do not depend on framework composition. This approximation has been shown to result in enthalpy deviations of only 1 kJ/mol at 623 K.²⁷

Three zeotype topologies exhibiting different channel and cavity structures were studied.³¹ The AlPO-34/CHA frameworks having eight-membered pores and large cavities were represented by periodic 36T hexagonal cell. The AlPO-18/AEI frameworks were represented by periodic 48T cell, having a different cavity structure connected by eight-membered pores. The AlPO-5/AFI has straight twelve-membered pore channel, and it was represented by 48T sites in a super cell constructed by repeating the unit cell twice in direction of the channel. The optimized unit cell constants of the three frameworks are listed in Table S1. Substitutions of P (by Si, Ge, or Ti) or Al (by Mg, or Zn) in AlPO zeotypes or Si (by Al, or Ga) in zeolites generate one Brønsted acid site per unit cell. The Brønsted acid site is located at the O2 position in AlPO-34/CHA framework based on previous works,⁶⁵ between T2 and T1 sites in AlPO-18/AEI framework as it is the most stable site (see Table S2), and at

O atoms linking two 4-membered rings in AlPO-5/AFI as it is the site most accessible to methanol, respectively. The positions of all atoms were allowed to relax in the calculations while the lattice constants were fixed at the optimized values.

Acknowledgements. We gratefully acknowledge the support from the U.S. Department of Energy, Office of Sciences, Office of Basic Energy Sciences to the SUNCAT Center for Interface Science and Catalysis. C.-M.W. acknowledges financial support from the National Science Foundation of China (21103231) and SINOPEC. The authors would like to thank Jens K. Nørskov for fruitful discussions.

Supporting information.

Electronic supplementary information (ESI) available. See DOI:

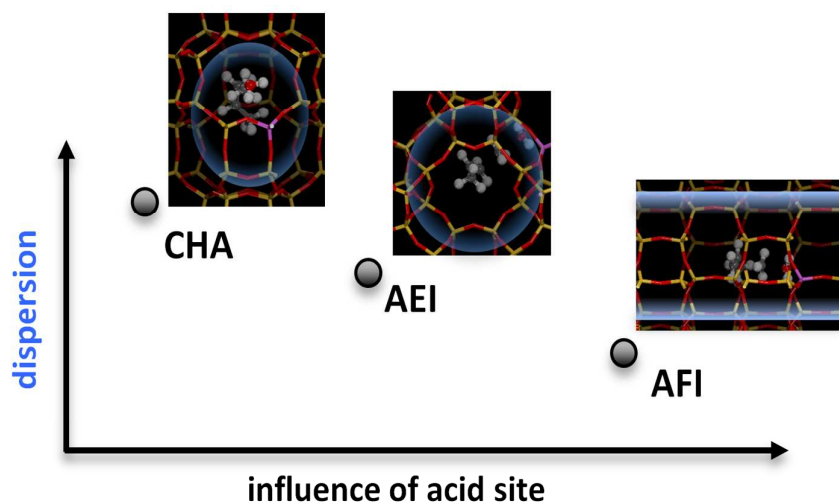
References

- 1 A. Corma, *J. Catal.*, 2003, **216**, 298-312.
- 2 W. Vermeiren and J. P. Gilson, *Top. Catal.*, 2009, **52**, 1131-1161.
- 3 C. D. Chang, *Catal. Rev. Sci. Eng.*, 1983, **25**, 1-118.
- 4 M. Stocker, *Micropor. and Mesopor. Mater.*, 1999, **29**, 3-48.
- 5 R. A. Van Santen and G. J. Kramer, *Chem. Rev.*, 1995, **95**, 637-660.
- 6 J. F. Haw, *Phys. Chem. Chem. Phys.*, 2002, **4**, 5431-5441.
- 7 M. Brandle and J. Sauer, *J. Am. Chem. Soc.*, 1998, **120**, 1556-1570.
- 8 A. Bhan and E. Iglesia, *Acc. Chem. Res.*, 2008, **41**, 559-567.
- 9 R. Gounder and E. Iglesia, *Acc. Chem. Res.*, 2011, **45**, 229-238.
- 10 D. A. Simonetti, R. T. Carr and E. Iglesia, *J. Catal.*, 2012, **285**, 19-30.
- 11 A. J. Jones, S. I. Zones and E. Iglesia, *J. Phys. Chem. C*, 2014, **118**, 17787-17800.
- 12 M. Mazar, S. Al-Hashimi, A. Bhan and M. Cococcioni, *J. Phys. Chem. C*, 2012, **116**, 19385-19395.
- 13 A. J. Jones, R. T. Carr, S. I. Zones and E. Iglesia, *J. Catal.*, 2014, **312**, 58-68.
- 14 J. K. Nørskov, T. Bligaard, J. Rossmeisl and C. H. Christensen, *Nat. Chem.*, 2009, **1**, 37-46.
- 15 J. K. Nørskov, F. Abild-Pedersen, F. Studt and T. Bligaard, *Proc. Nat. Acad. Sci.*, 2011, **108**, 937-943.
- 16 F. Studt, F. Abild-Pedersen, T. Bligaard, R. Z. Sørgensen, C. H. Christensen and J. K. Nørskov, *Science*, 2008, **320**, 1320-1322.
- 17 J. Greeley, T. F. Jaramillo, J. Bonde, I. Chorkendorff and J. K. Nørskov, *Nat. Mater.*, 2006, **5**, 909-913.
- 18 F. Studt, I. Sharafutdinov, F. Abild-Pedersen, C. F. Elkjaer, J. S. Hummelshøj, S. Dahl, I. Chorkendorff and J. K. Nørskov, *Nat. Chem.*, 2014, **6**, 320-324.
- 19 S. Alayoglu, A. U. Nilekar, M. Mavrikakis and B. Eichhorn, *Nat. Mater.*, 2008, **7**, 333-338.
- 20 P. Borges, R. Ramos Pinto, M. Lemos, F. Lemos, J. Védrine, E. Derouane and F. Ramôa Ribeiro,

- J. Mol. Catal. A: Chem.*, 2005, **229**, 127-135.
- 21 N. Katada, K. Suzuki, T. Noda, G. Sastre and M. Niwa, *J. Phys. Chem. C*, 2009, **113**, 19208-19217.
- 22 E. A. Pidko and R. A. van Santen, *J. Phys. Chem. C*, 2009, **113**, 4246-4249.
- 23 P. Deshlahra, R. T. Carr and E. Iglesia, *J. Am. Chem. Soc.*, 2014, **136**, 15229-15247.
- 24 M. Boronat and A. Corma, *Catal. Lett.*, 2015, **145**, 162-172.
- 25 J. Sauer and M. Sierka, *J. Comput. Chem.*, 2000, **21**, 1470-1493.
- 26 R. T. Carr, M. Neurock and E. Iglesia, *J. Catal.*, 2011, **278**, 78-93.
- 27 C. M. Wang, R. Y. Brogaard, B. M. Weckhuysen, J. K. Nørskov and F. Studt, *J. Phys. Chem. Lett.*, 2014, 1516-1521.
- 28 A. Auroux, *Top. Catal.*, 2002, **19**, 205-213.
- 29 E. Derouane, J. C. Vadrine, R. R. Pinto, P. Borges, L. Costa, M. Lemos, F. Lemos and F. R. Ribeiro, *Catal. Rev. Sci. Eng.*, 2013, **55**, 454-515.
- 30 R. Y. Brogaard, C. M. Wang and F. Studt, *ACS Catal.*, 2014, **4**, 4504-4509.
- 31 C. Baerlocher, L. B. McCusker and D. H. Olson, *Atlas of zeolite framework types*, Elsevier, 2007.
- 32 J. Wellendorff, K. T. Lundgaard, A. Møgelhøj, V. Petzold, D. D. Landis, J. K. Nørskov, T. Bligaard and K. W. Jacobsen, *Phys. Rev. B*, 2012, **85**, 235149.
- 33 R. Y. Brogaard, P. G. Moses and J. K. Nørskov, *Catal. Lett.*, 2012, **142**, 1057-1060.
- 34 R. Y. Brogaard, R. Henry, Y. Schuurman, A. J. Medford, P. G. Moses, P. Beato, S. Svelle, J. K. Nørskov and U. Olsbye, *J. Catal.*, 2014, **314**, 159-169.
- 35 K. Suzuki, G. Sastre, N. Katada and M. Niwa, *Phys. Chem. Chem. Phys.*, 2007, **9**, 5980-5987.
- 36 A. J. Medford, J. Wellendorff, A. Vojvodic, F. Studt, F. Abild-Pedersen, K. W. Jacobsen, T. Bligaard, J. K. Nørskov, *Science*, 2014, **345**, 197-200.
- 37 J. Chen, P. Wright, S. Natarajan and J. Thomas, *Stud. Surf. Sci. Catal.*, 1994, **84**, 1731-1738.
- 38 U. Olsbye, S. Svelle, M. Bjorgen, P. Beato, T. V. W. Janssens, F. Joensen, S. Bordiga and K. P. Lillerud, *Angew. Chem. Int. Ed.*, 2012, **51**, 5810-5831.
- 39 V. Van Speybroeck, K. De Wispelaere, J. Van der Mynsbrugge, M. Vandichel, K. Hemelsoet and M. Waroquier, *Chem. Soc. Rev.*, 2014, **43**, 7326-7357.
- 40 S. Svelle, C. Tuma, X. Rozanska, T. Kerber and J. Sauer, *J. Am. Chem. Soc.*, 2009, **131**, 816-825.
- 41 S. Svelle, P. O. Ronning, U. Olsbye and S. Kolboe, *J. Catal.*, 2005, **234**, 385-400.
- 42 S. Svelle, P. A. Ronning and S. Kolboe, *J. Catal.*, 2004, **224**, 115-123.
- 43 K. Hemelsoet, J. Van der Mynsbrugge, K. De Wispelaere, M. Waroquier and V. Van Speybroeck, *ChemPhysChem*, 2013, **14**, 1526-1545.
- 44 J. Van der Mynsbrugge, J. De Ridder, K. Hemelsoet, M. Waroquier and V. Van Speybroeck, *Chem. Eur. J.*, 2013, **19**, 11568-11576.
- 45 S. Ilias and A. Bhan, *ACS Catal.*, 2012, **3**, 18-31.
- 46 C. M. Wang, Y. D. Wang, Z. K. Xie and Z. P. Liu, *J. Phys. Chem. C*, 2009, **113**, 4584-4591.
- 47 C. M. Wang, Y. D. Wang, H. X. Liu, Z. K. Xie and Z. P. Liu, *J. Catal.*, 2010, **271**, 386-391.
- 48 C. M. Wang, Y. D. Wang and Z. K. Xie, *J. Catal.*, 2013, **301**, 8-19.
- 49 I. M. Hill, S. Al Hashimi and A. Bhan, *J. Catal.*, 2012, **285**, 115-123.
- 50 S. Svelle, F. Joensen, J. Nerlov, U. Olsbye, K. P. Lillerud, S. Kolboe and M. Bjorgen, *J. Am. Chem. Soc.*, 2006, **128**, 14770-14771.
- 51 C. M. Wang, Y. D. Wang and Z. K. Xie, *Catal. Sci. Tech.*, 2014, **4**, 2631-2638.

- 52 S. Svelle, M. Visur, U. Olsbye and M. Bjørgen, *Top. Catal.*, 2011, **54**, 897-906.
- 53 T. Maihom, B. Boekfa, J. Sirijaraensre, T. Nanok, M. Probst and J. Limtrakul, *J. Phys. Chem. C*, 2009, **113**, 6654-6662.
- 54 J. Van der Mynsbrugge, S. L. Moors, K. De Wispelaere and V. Van Speybroeck, *ChemCatChem*, 2014, **6**, 1906-1918.
- 55 J. Gomes, M. Head-Gordon and A. T. Bell, *J. Phys. Chem. C*, 2014, **118**, 21409-21419.
- 56 A. M. Vos, K. H. Nulens, F. De Proft, R. A. Schoonheydt and P. Geerlings, *J. Phys. Chem. B*, 2002, **106**, 2026-2034.
- 57 V. Van Speybroeck, J. Van der Mynsbrugge, M. Vandichel, K. Hemelsoet, D. Lesthaeghe, A. Ghysels, G. B. Marin and M. Waroquier, *J. Am. Chem. Soc.*, 2011, **133**, 888-899.
- 58 C. Jarque and A. Buckingham, *Chem. Phys. Lett.*, 1989, **164**, 485-490.
- 59 F. Eder and J. A. Lercher, *Zeolites*, 1997, **18**, 75-81.
- 60 B. A. De Moor, M. F. Reyniers, O. C. Gobin, J. A. Lercher and G. B. Marin, *J. Phys. Chem. C*, 2011, **115**, 1204-1219.
- 61 S. Jakobtorweihen, N. Hansen and F. J. Keil, *Mol. Phys.*, 2005, **103**, 471-489.
- 62 J. Enkovaara, C. Rostgaard, J. J. Mortensen, J. Chen, M. Dulak, L. Ferrighi, J. Gavnholt, C. Glinsvad, V. Haikola, H. A. Hansen, H. H. Kristoffersen, M. Kuisma, A. H. Larsen, L. Lehtovaara, M. Ljungberg, O. Lopez-Acevedo, P. G. Moses, J. Ojanen, T. Olsen, V. Petzold, N. A. Romero, J. Stausholm-Moller, M. Strange, G. A. Tritsarlis, M. Vanin, M. Walter, B. Hammer, H. Hakkinen, G. K. H. Madsen, R. M. Nieminen, J. Norskov, M. Puska, T. T. Rantala, J. Schiøtz, K. S. Thygesen and K. W. Jacobsen, *Journal of Physics-Condensed Matter*, 2010, **22**, 253202.
- 63 P. E. Blochl, *Phys. Rev. B*, 1994, **50**, 17953-17979.
- 64 G. Henkelman, B. P. Uberuaga and H. Jónsson, *J. Chem. Phys.*, 2000, **113**, 9901-9904.
- 65 K. Hemelsoet, A. Nollet, V. Van Speybroeck and M. Waroquier, *Chem. Eur. J.*, 2011, **17**, 9083-9093.

Table of Contents



Transition-state enthalpies in olefin-methanol reactions scale linearly with ammonia adsorption enthalpy as descriptor of acid site reactivity in zeolite catalysis. The slopes of these scaling relations vary with dispersion interaction with the framework.